Chin. J. Astron. Astrophys. Vol. 6 (2006), **Suppl. 2**, 228–232
(*http://www.chjaa.org*)

Chinese Journal of
Astronomy and
Astrophysics

Dissipation of Low-Frequency Waves in the Pulsar Wind

Qinghuan Luo ⋆

School of Physics, University of Sydney, NSW 2006, Australia

Abstract Low-frequency waves and energy dissipation in the relativistic pulsar wind are discussed. The Poynting flux, which is initially dominant in the pulsar wind, may be transported by large amplitude low-frequency waves: in the region near the pulsar such waves can be relativistic MHD waves, and in the region far from the pulsar they can be electromagnetic (EM) waves. Both types of wave are considered and in the latter case, coherent nonlinear Compton scattering may lead to highly beamed coherent radio emission with synchrotron-like spectra, which may be potentially observable.

Key words: pulsar — particle acceleration — radiation mechanism: nonthermal

1 INTRODUCTION

A major unresolved issue in understanding phenomena of pulsar wind nebulae (PWNe) is how the pulsar's spin-down power is converted to particle kinetic energy in the relativistic wind that interacts with its environment. The pulsar's rotation energy drives a relativistic outflow that is electromagnetically dominant near the star and terminates at the standing shock where the flow becomes nonrelativistic. The features of the termination shock are well studied in observations from radio to X-rays (Hester et al. 1995) and formation of such shock requires the energy content of the wind before the shock to be predominantly in kinetic energy (Kennel & Coroniti 1984). Numerous mechanisms have been proposed to explain such conversion, and these can be broadly classified as the steady MHD wind model in which the wind is treated as steady ideal MHD fluids (e.g. Michel 1969; Chiueh, Li & Begelman 1998), and the plasma wind model in which modulation due to the magnetic dipole's rotation plays an essential role in energy transport and dissipation (e.g. Asseo, Kennel & Pellat 1978; Usov 1994; Melatos & Melrose 1996; Lyubarsky & Kirk 2001; Kirk & Skjaeraasen 2003). In the ideal MHD model, the conversion of Poynting flux to kinetic energy is achieved through collimation, which is possible under certain special boundary conditions at the base of the outflow (e.g. Chiueh, Li & Begelman 1998). In the plasma wind model, the Poynting flux is transported in large amplitude waves and dissipated through magnetic reconnection near the equatorial region if the large amplitude waves concerned are the entropy wave (e.g. Lyubarsky & Kirk 2001) or through wave damping if the Poynting flux is carried by EM waves (e.g. Asseo, Kennel & Pellat 1978).

The low-frequency waves play an essential role in energy transport and dissipation in the pulsar wind. The idea that a pulsar emits large amplitude waves was first discussed by Ostriker & Gunn (1969) and was not favored initially because a pulsar generates ample relativistic pairs and EM waves at pulsar's rotation frequency do not propagate in the dense pair plasma. However, there are two main arguments for the relevance of low-frequency waves in the pulsar wind. First, observations of the outward-propagating features in the Crab nebula, known as wisps, in both radio and optical strongly point to the wave-like nature of the pulsar wind (Bietenholz et al. 2004). Second, the pulsar's rotation should modulate its outflow, generating waves that can transport energy and be dissipated. Such waves can be MHD waves that can propagate in a dense plasma and be dissipated or converted to EM waves. Large amplitude EM waves may exist beyond a certain radial distance where the plasma density becomes sufficiently low. The relevant large amplitude MHD waves and EM waves in the pulsar wind are discussed here focusing on dissipation of and coupling

⋆ E-mail: luo@physics.usyd.edu.au

between the two types of wave. Specifically, nonlinear Compton scattering of relativistic particles on large amplitude waves is considered, as it may provide observable signatures for the existence of such EM waves.

2 THE σ PROBLEM IN PULSAR WINDS

The pulsar light cylinder radius (LC), $R_{\rm LC}$, which is the radius where the rotation speed equals the speed of light, separates two regions: the magnetosphere in which the magnetic field as the zeroth order approximation is considered as a static dipole and the wind in which the toroidal magnetic field component becomes important. One may define a characteristic radius, r_*, where the toroidal field becomes dominant and particles move radially. This radius is generally different from $R_{\rm LC}$. However, except where it is specified otherwise, for simplicity, $r_* \sim R_{\rm LC}$ is assumed. The properties of the wind can be characterised by a parameter, σ, the ratio of the magnetic to particle kinetic energy, defined by

$$\sigma = \frac{B^2}{2\mu_0 n m_e c^2 \gamma}, \tag{1}$$

where γ is the Lorentz factor of the bulk plasma, $n = M n_{\rm GJ}$ is the pair density in terms of the multiplicity M (number of pairs per primary particle) and the Goldreich-Julian (GJ) density $n_{\rm GJ} = \varepsilon_0 \Omega B/e$. The GJ density inside the LC can be written as $n_{\rm GJ} = N_{\rm GJ}(R_0/r)^3$, where r is a radial distance, $R_0 = 10^4\,{\rm m}$ is the star's radius, and $N_{\rm GJ} \approx 5.3 \times 10^{18}(B_0/5 \times 10^8\,{\rm T})(P/33\,{\rm ms})^{-1}\,{\rm m}^{-3}$ is the GJ density on the polar cap (PC). Alternatively, Equation (1) can be written as the ratio of the electron cyclotron frequency to rotation frequency Ω: $\sigma = (\Omega_e/2\gamma M\Omega)|_{r=R_{\rm LC}}$. For the Crab pulsar, one predicts that $\sigma \sim 10^3 - 10^4$ at the LC. Since both the plasma density and the magnetic energy density are scaled as $1/r^2$, σ would remain constant if there were no dissipation in the wind. Since from observations one infers a low $\sigma \ll 1$ before the termination shock (Kennel & Coroniti 1984; Hester et al. 1995), there must be a conversion mechanism that transforms the magnetic energy to particle's kinetic energy. One strong possibility is through dissipation of large amplitude waves.

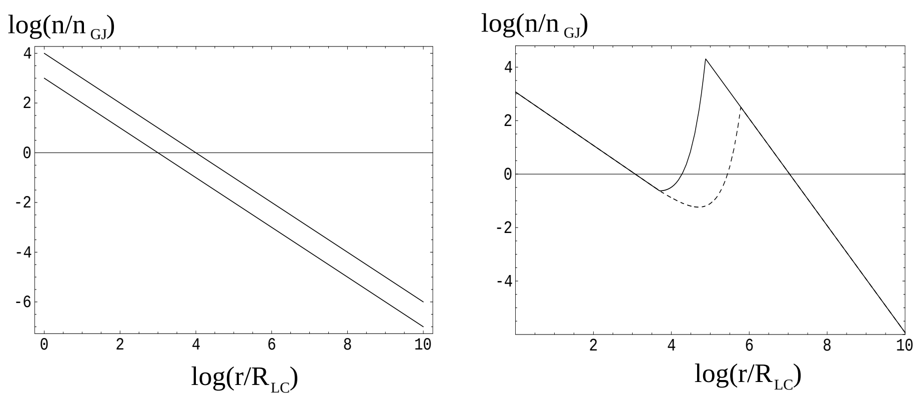

Fig. 1 The ratio of the plasma number density to the critical density for $M = 10^3$ (lower) and 10^4 (upper). Left: Absence of damping. Right: Damping is included. We assume damping occurs at $r = 10^3 R_{\rm LC}$ with the characteristic damping length $\Delta r = r$ (solid line) and $10r$ (the dashed line). The inclusion of damping leads to a second critical radius where $n = n_{\rm GJ}$. The parameters are for the Crab pulsar. The MHD and EM zones correspond respectively to the regions with $n/n_{\rm GJ} \geq 1$ and $n/n_{\rm GJ} < 1$.

3 LARGE AMPLITUDE WAVES

The pulsar wind is commonly described in the ideal MHD model, often in the steady flow approximation. However, it was recognised that the ideal MHD conditions can only be satisfied up to a certain radial distance before the plasma density drops to a sufficiently low value below which the displacement current cannot be neutralised (e.g. Usov 1994; Melatos & Melrose 1996). The corresponding critical density n_c

can be estimated as follows. The displacement current (the $\partial \boldsymbol{E}/\partial t$ term in the Maxwell's equations) is $\sim \Omega E/\mu_0 c^2$, where E is the electric field of the relevant wave. The current supported by a relativistic plasma is about nec. Assuming $E \sim cB$, one finds the critical density as

$$n_c = \varepsilon_0 B\Omega/e = n_{\rm GJ}, \tag{2}$$

which decreases with an increasing radial distance as $1/r$, much slower than the plasma density does as $1/r^2$, where the wave frequency Ω is identified as the pulsar angular frequency. It should be emphasised here that n_{GJ} has a different meaning from that for the magnetosphere: It characterises the displacement current of a wave not the density for corotation as in the magnetosphere, though they both have the same form. Let $n_{\rm GJ} = n_{\rm GJ}(r_*)(r_*/r)^2$ for $r > r_* \geq R_{\rm LC}$ and $n = Mn_{\rm GJ}$. When $r_* \sim R_{\rm LC}$, one has $n_{\rm GJ}(r_*) \sim N_{\rm GJ}\theta_d^6$, where $\theta_d = (R_0/R_{\rm LC})^{1/2}$ is the half-opening angle of the PC. Using $n_c = n_{\rm GJ}(r_1)(r_*/r)$, the critical density corresponds to a radius,

$$r_c = M\, r_*. \tag{3}$$

For $M = 5 \times 10^3$, one has $r_c \sim 5 \times 10^3 R_{\rm LC}$ for $r_* = R_{\rm LC}$, well inside the termination shock ($r_s \sim 7 \times 10^{16}\,{\rm m}$). The other useful characteristic radius is where $\Omega = \omega_p$, given by $r_1/R_{\rm LC} = 2.2 \times 10^7\,(P/33\,{\rm ms})^{-1}(B_0/5 \times 10^8\,{\rm T})^{1/2}(M/5 \times 10^3)^{1/2}$, giving rise to $r_1 \sim 10^{13}\,{\rm m}$ for the Crab pulsar. Figure 1 shows plots of the ratio of the plasma density to the critical density. The relativistic flow at $r \geq r_c$ must be treated as EM waves (e.g. Usov 1994; Melatos & Melrose 1996).

If the relevant EM wave is subject to damping, the above simple two-zone model does not apply. The critical density depends on the wave amplitude and damping would effectively increase the critical density. This complication is illustrated in Figure 1. One assumes that the wave is damped on a characteristic length Δr. In each case there are two MHD zones and two EM wave zones. The outer EM zone is determined by r_1 and the size of the inner EM zone strongly dependent on the damping rate and also on how MHD waves couple to an EM wave and vice versa. In the first MHD zone $r \leq r_c$, EM waves cannot propagate (Asseo, Kennel & Pellat 1978). Poynting flux may be carried in relativistic MHD waves such as entropy waves or fast magnetosonic waves (e.g. Lou 1998; Lyubarsky 2003), and these waves may be subject to some dissipation due to turbulences by reducing the displacement current, or converted to EM waves, which are damped at a larger radial distance near the second critical radius (see Figure 1). Asseo et al considered damping of large amplitude electromagnetic waves in the fluid model including radiation reaction and found that the damping distance is $\propto (n_{\rm GJ}/n)^3$, implying that large amplitude waves are damped only when the density is close to the critical density (2). Thus it seems possible that the dissipation is only partial and some vacuum-like, large amplitude waves may exist in the EM zones.

4 NONLINEAR COMPTON SCATTERING

If large amplitude EM waves exist in a particular region in the pulsar wind, such as the EM wave zones described above, nonlinear Compton scattering by relativistic electrons or positrons may produce observable radiation (Blandford 1972; Arons 1972). For electrons (or positrons) the basic dimensionless parameter characterising the strength of the radiation field is

$$a = \frac{eE}{m_e c\Omega} \approx 10^{11}\left(\frac{P}{33\,{\rm ms}}\right)^{-3}\left(\frac{B}{10^8\,{\rm T}}\right)\left(\frac{R_{\rm LC}}{r}\right), \tag{4}$$

where E is the amplitude of the electric field of the wave, and the approximation corresponds to the assumption of transverse waves with $E \sim cB$. The basic theory for Compton scattering on an intense radiation field was worked out between late 60 s and early 70 s (e.g. Eberly & Sleeper 1968; Sarachik & Schappert 1970; Gunn & Ostriker 1971) and was refined recently, primarily motivated by the recent advances in high power laser technology (e.g. Esarey, Ride & Sprangle 1993). There are two approaches in treating Compton scattering on intense radiation fields: a test particle model (Sarachik & Schappert 1970; Gunn & Ostriker 1971; Blandford 1972; Arons 1972), in which motion of a single particle in a background radiation field is considered, and fluid model (e.g. Asseo, Kennel & Pellat 1978). In the following we adopt the former with the wave-induced space-charge potential Φ derived from the fluid continuity equation and the Poisson equation (Sprangle et al. 1992). An exact solution can be obtained assuming that the wave amplitude is a periodic function of a Lorentz invariant phase $\phi = \Omega t - \boldsymbol{k}_0 \cdot \boldsymbol{x}$, where $\boldsymbol{k}_0$ is the wave vector of the incoming (large amplitude) wave.

The electric field and power radiated by a particle in a strong radiation field can be derived from the current

$$\boldsymbol{j}(\omega, \boldsymbol{k}) = \frac{ec}{\Omega \tilde{D}_0} e^{i\varphi_0} \int d\phi \, \boldsymbol{u}(\phi) \exp\left[i\left(A\phi - Z\sin\phi\right)\right], \tag{5}$$

where ω and $\boldsymbol{k} = k(\sin\theta, 0, \cos\theta)$ are the frequency and wave vector of the scattered radiation, respectively. In Equation (5), $\varphi_0 = k(1-\cos\theta)z_0$ is the phase due to the initial position, $\tilde{D}_0 = D_0 + \hat{\Phi}$, $\hat{\Phi} = \Phi/m_e c^2$, $D_0 = \gamma_0(1 - \boldsymbol{n}_0 \cdot \boldsymbol{\beta}_0)$ with $\boldsymbol{n}_0 = \boldsymbol{k}_0 c/\Omega$ is the doppler factor, $A = (\omega/\Omega)\left[1 + (1-\cos\theta)(1 + a^2 - \tilde{D}_0^2)/2\tilde{D}_0^2\right]$, and $Z = k(\rho\sin\theta + x_0)$. Equation (5) is derived using the single particle approach (Melrose 1986). We assume that the particle moves initially along the z axis and that the waves are circularly polarised, propagating in the same direction (the z axis). The current can be evaluated by expanding the exponential function in terms of Bessel functions. There are two distinct features for scattering involving intense radiation fields. First, scattering on an intense radiation field is intrinsically anisotropic, in contrast to the usual Thomson scattering that has symmetry in between backward and forward scattering. Second, because of the relativistic effect the scattered radiation is similar to synchrotron radiation with the characteristic frequency $\omega_c \sim 2a^3\Omega$ (while for the conventional Compton scattering, one has $\omega_c \sim 2\tilde{D}_0^2\Omega$).

In an intense radiation field $a \gg 1$, a particle initially at rest can be accelerated instantly to relativistic energy and the radiation is always beamed approximately in the direction of the incident waves at an angle determined from

$$\cos\theta_c = 1 - \frac{2\tilde{D}_0^2}{1 + a^2 + \tilde{D}_0^2}. \tag{6}$$

Note that the critical angle is determined by the drift velocity $\beta_D \equiv (1 + a^2 - \tilde{D}_0^2)/(1 + a^2 + \tilde{D}_0^2)$. When the effect of space charges induced by the wave is ignored ($\Phi = 0$), which is applicable for a primary beam, one has $\tilde{D}_0 = D_0 = \gamma_0(1-\beta_0) \approx 1/2\gamma_0$ and obtains $\theta_c \sim 1/a\gamma_0$. Emission due to nonlinear Compton scattering is confined to a very narrow cone about $\theta_c \ll 1$.

5 COHERENT RADIO EMISSION

Intense coherent radio emission may be produced through coherent Compton scattering on low-frequency large amplitude waves. The total radiation is said to be coherent if the wave amplitudes from individual particles are added together constructively, i.e. all particles act collectively as a single macrocharge $N_c e$, emitting a total power of N_c^2 times that of a single particle. Consider the scattered radiation in the direction $\theta \sim 0$. From (5), one may obtain the condition for coherent scattering as $2|\varphi_{0i} - \varphi_{0j}| < 1$, corresponding to $\Delta z/\lambda_0 < (\lambda a^6/\lambda_0)(\Omega/\omega_p)^2$, where φ_{0i} and z_{0i} are the ith particle's initial phase and position, as defined in (5), $\Delta z = |z_{0i} - z_{0j}|$, $\lambda = c/\omega$, and $\lambda_0 = c/\Omega \sim 10^8\,\mathrm{cm}$ for the Crab pulsar. Thus, for forward scattering, the effective coherence length can be comparable to the incoming wavelength λ_0.

Coherent Compton scattering works for both an electron (or positron) beam and a neutral plasma. Since the pair plasma in the wind has a very broad distribution in momentum, a coherent bunch can be dispersed on a time much shorter than the flight time to the standing shock. Thus we only consider the case of a primary electron (or positron) beam extracted from the PC. In the PC model, primary particles (electrons or protons) are accelerated to ultrarelativistic energy. If acceleration is transient and time dependent, these primary particles form clouds of a typical size $L_g = t_a/c \sim 10^2\,\mathrm{m}$, where t_a is the light crossing time in the acceleration, typically about $t_a \sim 3 \times 10^{-5}\,\mathrm{s}$ for $L_g = 10^2\,\mathrm{m}$. The number of particles in a bunch of a longitudinal size L_c is about $N_c \approx 4\pi\eta L_c N_{\rm GJ}\theta_d^6 R_{\rm LC}^2 \approx 4.2 \times 10^{31}\eta\left(L_c/10^6\,\mathrm{m}\right)(P/33\,\mathrm{ms})^{-2}\left(B_0/5\times10^8\,\mathrm{T}\right)$, where $\eta < 1$ is a parameter characterising the transverse coherence size. Since $L_c \gg L_g$, a bunch contains a large number (L_c/L_g) of clouds and the above estimate should be modified by a filling factor (< 1) that for simplicity is ignored here. If the transverse size is assumed to be $r/\gamma_0 a$, where r is the radial distance to the emission region, one has $\eta \sim 1/(\gamma_0 a)^2 \sim 4 \times 10^{-18}$ for $\gamma_0 = 10^6$ and $a = 500$. This gives $N_c \sim 10^{14}$. It is a good approximation to treat the accelerated primary particles as nearly monoenergetic with a Lorentz factor γ_0 and a small spread $\Delta\gamma \ll \gamma_0$. It can be shown that the effect of the velocity dispersion on the coherence can be ignored. The dispersion time corresponds to the time for two particles to drift apart over the distance L_c, which can be estimated from $t_c \sim 2\gamma_0^3 L_c/\Delta\gamma c \approx 10^8\,\mathrm{s}$. For $\gamma_0 = 10^6$, this time is much longer than the flight time to the termination shock.

The power radiated by an electron is $P_s \approx e^2ck_0^2a^2\gamma_0^2(1-\beta_0)^2 \approx e^2ck_0^2a^2/4\gamma_0^2$, which can be derived from (5). The emissivity is estimated to be $N_c^2P_s/\Delta V$ with $\Delta V = (r/\gamma_0 a)^2\Delta r$ is the emitting volume and Δr is the depth of the emission region. As the received power is $(\gamma_0 a)^2$ times the power radiated due to relativistic beaming, the flux density at a distance D is estimated to be

$$F \approx \frac{N_c^2 P_s(\gamma_0 a)^4}{D^2 f_c}, \tag{7}$$

where f_c=$\omega_c/2\pi$. Notice that the basic angular width is $\Delta\theta < \theta_c \sim 1/a\gamma_0$, much smaller than that (the smallest possible $1/\gamma_0$) can be achieved within the magnetosphere. Since the relativistic wind is likely inhomogeneous in the transverse direction, which may be traced back to a nonuniform pair cascade across the polar cap, an extremely narrow beam structure modulated by pulsar's rotation can be observed if the transverse inhomogeneity in the scattering region has a characteristic length $r/\gamma_0 a$. The flux density from forward scattering is estimated to be $F \approx (0.2\,\mathrm{Jy})\ (D/2\,\mathrm{kpc})^{-2}\,(P/33\,\mathrm{ms})^{-10/3}\left(B_0/5\times10^8\,\mathrm{T}\right)^2\left(\gamma_0/10^6\right)^{-2}(f_c/1\,\mathrm{GHz})^{-1/3}$, where we use $a \sim (f_cP)^{1/3}$ and $L_c \sim \lambda_0 = c/\Omega$. For the Crab pulsar, $f_c = 1\,\mathrm{GHz}$ corresponds to $a \sim 300$. For the emission to be coherent, propagation of the incoming wave must be highly collimated with the flow of the scattering particles, implying that occurrence of such events may be infrequent.

6 CONCLUSIONS

Dissipation or conversion of the magnetic energy to particle's kinetic energy occurs in the form of large amplitude low-frequency waves. The relevant low-frequency waves near the LC are MHD waves, which can decay or couple to EM waves in the low plasma density regions. The known processes of dissipation of MHD waves are not efficient enough to achieve $\sigma \ll 1$. Thus, it is possible that MHD waves couple to EM waves and are damped subsequently. It is suggested here that existence of EM waves in the pulsar wind can be tested by detecting beamed coherent radio emission due to synchro-Compton radiation in the forward scattering regime.

References

Arons, J., 1972, ApJ, 177, 395
Asseo, E., Kennel, C. F., Pellat, R., 1978, A&A, 65, 401
Bietenholz, M. F., Hester, J. J., Frail, D. A., Bartel, N., 2004, ApJ, 615, 794
Blandford, R., 1972, A&A, 20, 135
Chiueh, T., Li, Z., Begelman, M., 1998, ApJ, 505, 835
Eberly, J. H., Sleeper, A., 1968, Phys. Rev. 176, 1570
Gunn, J. E., Ostriker, J. P., 1971, ApJ, 166, 523
Hester, J. et al., 1995, ApJ, 448, 240
Kennel, C. F., Coroniti, F. V., 1984, ApJ, 283, 694
Kirk, J., Skjaeraasen, O., 2003, ApJ, 591, 366
Lou, Y. Q., 1998, MNRAS, 294, 443
Lyubarsky, Y., Kirk, J. G., 2001, ApJ, 547, 437
Lyubarsky, Y., 2003, MNRAS, 339, 765
Max, C., Perkins, F., 1972, Phys. Rev. Lett. 29, 1731
Melatos, A., Melrose, D. B., 1996, MNRAS, 279, 1168
Melrose, D. B., 1986, Instabilities in Space and Laboratory Plasmas, Cambridge University Press
Michel, F., 1969, ApJ, 158, 727
Ostriker, J. P., Gunn, J. E., 1969, ApJ, 157, 1395
Sarachik, E. S., Schappert, G., 1970, Phys. Rev. D1, 2738
Sprangle, P., Esarey, E., Krall, J., Joyce, G., 1992, Phys. Rev. Lett., 69, 2200
Usov, V. V., 1994, MNRAS, 267, 1035